Optical Emission Signatures of Dual Planar Magnetron Plasmas for TiO_2 Deposition*)

Michelle Marie S. VILLAMAYOR, Takashi NAKAJIMA[1)], Henry J. RAMOS and Motoi WADA[1)]

Plasma Physics Laboratory, National Institute of Physics, College of Science, University of the Philippines – Diliman, Quezon City 1101, Philippines

[1)]*Applied Physics Laboratory, Department of Engineering Kyotanabe Campus, Doshisha University, Kyoto, Japan*

(Received 6 December 2010 / Accepted 7 March 2011)

The dual planar magnetron (DPM) configuration features a mirror reactive magnetron sputtering system unlike that of a single planar unbalanced magnetron set-up. Optical emission signatures of a mixed species of oxygen and argon plasmas show a decrease in intensity peaks when only a single plane is biased. This manifests an oxide layer formation on the target for the single planar case thereby lowering the sputtering yield of the titanium target. No changes in emission intensity peaks are observed when the dual planes are biased. This is favorable for increasing the yield of sputtered titanium beneficial for raising the deposition rate of TiO_2 thin film. The DPM process exhibits the anatase and rutile phases of the synthesized TiO_2 films. The films are characterized by XRD, FE-SEM, reflectance and FTIR spectroscopy. Photo-reactive properties of the materials are also presented.

Keywords: magnetron sputtering, passivation, sputtering, thin film deposition, TiO_2

DOI: 10.1585/pfr.6.2406045

1. Introduction

Titanium dioxide, commonly known as titania, is a very interesting material in terms of its chemical and optical properties. It is resistant to chemical damage, transparent in the near-infrared and visible spectra, and possess a high refractive index. Application of TiO_2 depends on its anatase or rutile structure. The anatase phase is photochemically active and thus useful in solar cell applications and gas sensitive devices. Rutile TiO_2 has a high resistivity and dielectric constant making it useful as capacitors and in microelectronics. The properties of TiO_2 are dependent on plasma parameters, duration of synthesis, substrate temperature, and artifacts of the deposition machine [1–13].

Reactive magnetron sputtering is a common mechanism for preparing Ti compound thin films such as TiO_2. However, deposition problems arise when oxides are formed covering and poisoning the titanium target due to the inflow of oxygen gas.

To address this problem, the DPM is designed with two targets facing each other in a mirror configuration with two reactive planar magnetrons essentially driving the plasma. The configuration increases the titanium yield by a series of sputtering particles bouncing back and forth hitting the titanium targets. The DPM operates at low energies (175 W) without the need of substrate RF biasing and annealing [14].

Optical emission signatures of argon and oxygen plasma mixtures with a single plane biased are compared to the case of two planes biased. The latter signifies favourable conditions for TiO_2 deposition. Synthesized TiO_2 films by the DPM process exhibit the anatase and rutile phases. The thin films are characterized by XRD, FE-SEM, reflectance and FTIR spectroscopy. Photo-reactive properties of the materials are also presented.

2. Experiment

The DPM (Figure 1) is composed of two titanium target sources facing each other with two planar magnetrons. The target bias can be adjusted in series with a resistor and solenoid for stable operation. The vacuum chamber is evacuated by a rotary pump coupled to a turbo molecular pump. Pirani and ionization gauges monitor the working pressures for the experiment. Argon and Oxygen gases are fed via gas needle valves placed near the port where the Pirani gauge is mounted. A view port for plasma spectroscopic analysis is provided near the turbomolecular pump. The view port can be removed to accommodate a substrate heating device. The substrate holder inside the chamber is connected to a centering ring positioned along the top of the chamber by a 0.1 mm diameter tungsten wire

The machine is operated as a magnetron sputtering device. Two titanium targets are placed on a wall facing each other inside the chamber. On the outer side of the two titanium targets are magnets arranged to optimize the sputtering. Cylindrical magnets 6 kG on the surface, (1 cm diameter × 1 cm, stacked into 2) with its axial south facing the

author's e-mail: mvillamayor@nip.upd.edu.ph

*) This article is based on the presentation at the 20th International Toki Conference (ITC20).

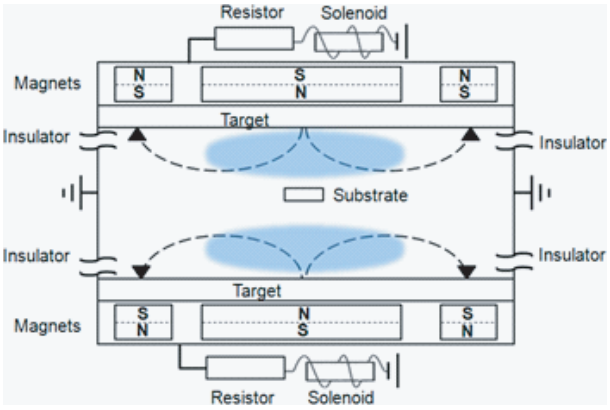

Fig. 1 The Dual Planar Magnetron.

inside of the vacuum chamber are aligned near the perimeter of the chamber target wall. North facing magnets are concentrated in the middle of the target wall. The other walls are insulated from the target walls and are grounded. In between the target walls is the substrate positioned parallel to the titanium faces.

Sample 1 was deposited with TiO_2 for 3 hours using the following conditions. Ar partial pressure was 0.7 Pa, and O_2 at 0.2 Pa. Plasma discharge current was set at 0.5 A while the discharge voltage was varied from −328 V to −356 V stepwise every 30 minutes. Sample 2 was synthesized under the same conditions but with heating. The heater was maintained at 300°C.

Sample 3 was deposited for six hours. The deposition process was run in two parts. For the first three hours, the Ar partial pressure was set at 0.7 Pa, and O_2 at 0.2 Pa. Plasma discharge current was set at 0.5 A with varying discharge voltage (−315 V to −341 V) changed every 30 minutes. O_2 was shut out for 3 minutes to enable Ar sputtering of the targets to remove the TiO_2 shield that may have been deposited on the target. Discharge voltage was changed from −341 V to −379 V every 30 seconds.

The remaining three hour deposition used 0.5 A discharge current, 0.7 Pa for Ar and 0.2 Pa for O_2 partial pressures. Discharge voltage was again gradually varied every 30 minutes from −259 V to −280 V.

Optical emission of the DPM with one planar target surface biased was compared with the mirror orientation where both targets were negatively biased. Gas partial pressures of O_2 and Argon was fed, monitored, and then adjusted to different settings.

Synthesized TiO_2 films were characterized by X-Ray Diffraction (XRD), field emission-scanning electron microscopy (FE-SEM), reflectance and Fourier transform infrared spectrometry (FTIR) reflectance. The photoresponse of the films were also measured.

3. Results and Discussions

Figure 2 a) is the optical spectra of the plasma inside the DPM with one target plane biased. The decrease in intensity of the peaks is noticeable as the partial pressures of O_2 and Ar gases are adjusted. As the partial pressure of oxygen is changed, an oxide layer poisons the target. High oxygen partial pressure leads to the deposition of TiO_2 onto the target which is unfavourable as it chokes the sputtering of titanium. To prevent the further deposition of TiO_2 oxygen gas feed must be cut off from the system to enable the Ar ions to sputter the walls and the target to dislodge the unwanted TiO_2 deposit. This is precisely what was done for sample 3 going through the process of argon cleaning although both targets were biased.

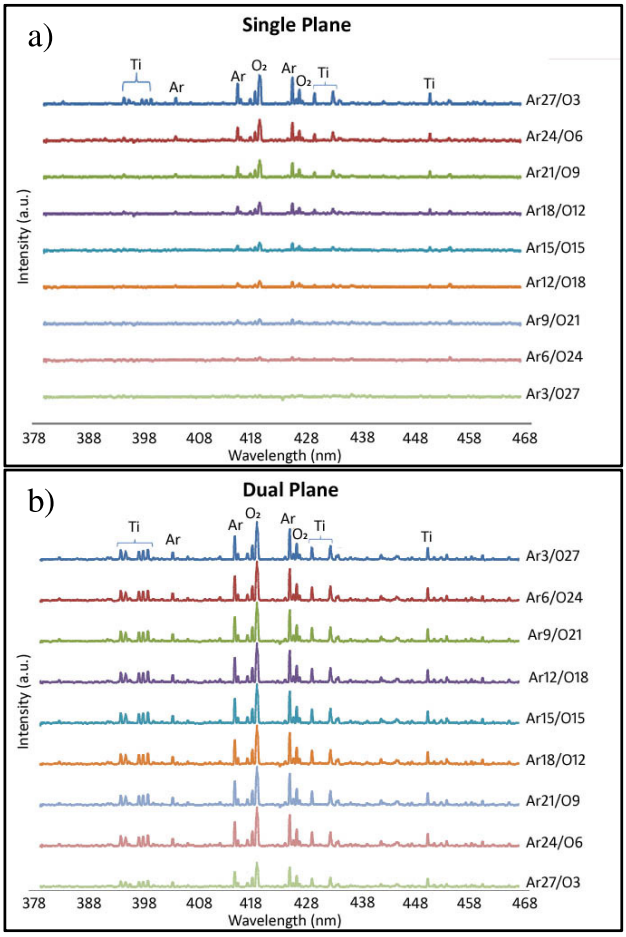

Fig. 2 Optical emission of the DPM at a) single plane biased and b) dual plane biased.

In Figure 2 b), the intensity peaks did not show any changes for the dual plane biased. This can be attributed to the mirror configuration preventing the two targets from becoming insulated. Argon ion together with the freed titanium particles bounce back and forth between the two mirrors enhancing the Ti sputter yield. The constant bombardment of the targets prevents the deposition of TiO_2 on both planes. The formation of TiO_2 on the targets insulates the targets. The unchanged optical emission intensity of the plasma as the gases are fed in the DPM means the targets are not being poisoned by TiO_2.

Figure 3 shows the effect of substrate heating and deposition time on the phases of the TiO_2 film. The XRD

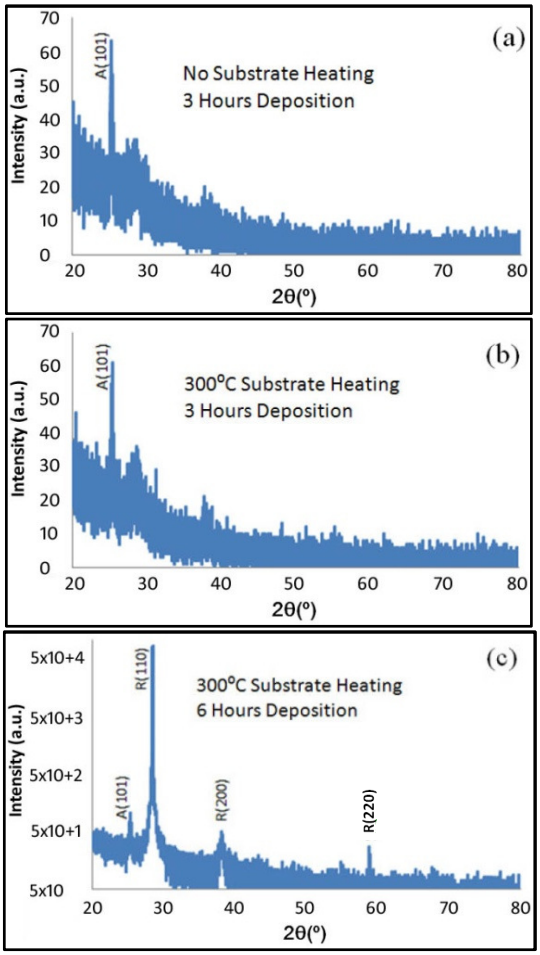

Fig. 3 XRD of (a) sample 1 and (b) sample 2 with predominantly anatase phase peak as compared to (c) sample 3 which is predominantly rutile phase.

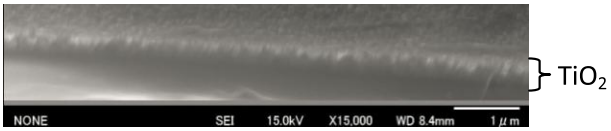

Fig. 4 FE-SEM of sample 3 with a thickness of 550 nm at 6 hours deposition. The deposition rate is ~1.53 nm/min.

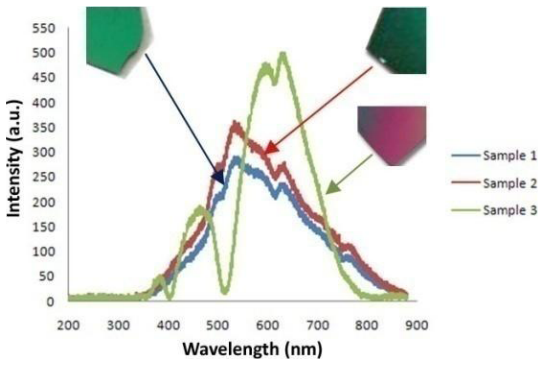

Fig. 5 Reflectance measurement of the three samples and their corresponding colours using visual images.

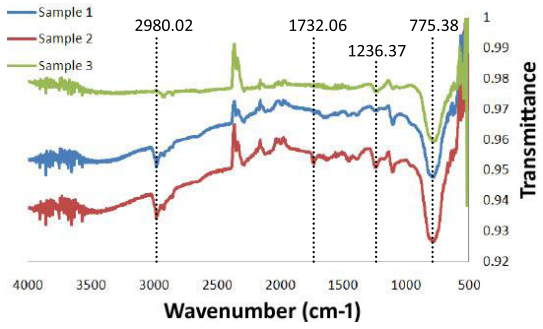

Fig. 6 FTIR measurement of the three samples.

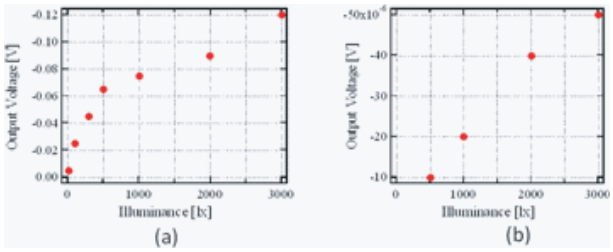

Fig. 7 Photo-response measurement of the two films where voltage is measured when a light source's illuminance is increased. (a) Sample 1 and (b) sample 3 were compared.

plots indicate no significant difference in the crystal structure for the first two samples. The TiO_2 film has the dominant anatase phase in both cases. At double the deposition time and substrate heating at 300°C the film crystalline structure shows the emergence of the rutile phases R(110), R(200) and R(220) aside from the anatase A(101). Si is the substrate used and it has dimensions of 2.5 cm × 2.5 cm × 0.3 mm.

The FE-SEM image of sample 3 is shown in Figure 4 with the layers labelled as TiO_2 and Si. The rate of TiO_2 formation is approximated at 1.53 nm/min with the film thickness at 550 nm deposited in six hours. The thickness of the films for samples 1 and 2 are estimated at 280 nm and 375 nm, respectively. The corresponding deposition rates are 1.55 nm/min and 2.08 nm/min, respectively.

Figure 5 shows the reflectance measurements of the three samples. Visual inspection has sample 1 peaking at the green wavelength. Sample 2 peaks somewhat at the same wavelength with a little higher intensity. Sample 3 has a high intensity peak near the red visible wavelength. FTIR signatures of the three samples are captured in Figure 6. Samples 1 and 2 have similar signatures with a decreased percent transmission greater than wavenumber 2000 cm^{-1} because they are anatase-dominant, as compared to sample 3 which is rutile-dominant. Absence of the dips at wavenumbers 2980.02 cm^{-1} and 1732.06 cm^{-1} are observed on the FTIR peak of sample 3.

Photo-responses of the samples 1 and 3 are shown in Figure 7. The negative value of the output voltage in

Figure 7 is due to the negative ion desorption [15] during the photoresponse measurement. The rate of negative ion desorption is proportional to the square root or linear function of the light flux for the anatase (Fig. 7 (a) and rutile (Fig. 7 (b) phase, respectively. The sample has been kept awhile before characterization. It is most likely that chemisorbed oxygen has set-in in the sample.

4. Conclusion

The dual planar magnetron is an effective TiO_2 fabricating device with enhanced deposition rate due to its mirrored-target design. For the two planar targets biased, the gas flow ratio of Ar:O_2 between 4:1 and 1:9 gives optical emission peaks without any significant difference as seen in the optical spectra. Anatase TiO_2 appears dominant at 3 hours deposition while the rutile phase requires longer deposition. The rate of formation of TiO_2 anatase was increased when substrate heating at 300°C was introduced. Reflectance and FTIR tests indicate the difference of the rutile and anatase dominant peaks and correlate, with the visual colour. The photo-response measurement of the device showed the higher magnitude of the output voltage of anatase compared to rutile.

[1] X. Chen and S.S. Mao, Chem. Rev. **107**, 2891 (2007).
[2] B. O'Regan and M. Grätzel, Nature **353**, 737 (24 October 1991).
[3] C.J. Tavares, J. Viera *et al.*, Materials Science and Engineering B **138**, 139 (2007).
[4] A. Fujishima and K. Honda, Nature **238**, 37 (1972).
[5] L. Mao, S. Tanemura *et al.*, Journal of Crystal Growth **260**, 118 (2004).
[6] S. Chaiyakun, A. Pokaipisit *et al.*, Applied Physics A **95**, 579 (2009).
[7] J. Zhao, X. Wang, R. Chen and L. Li, Solid State Communications **134**, 705 (2005).
[8] H.K. Yu, T.H. Eun, G. Yi and S. Yang, Journal of Colloid and Interface Science **316**, 175 (2007).
[9] K. Kalantar-zadeh *et al.*, Thin Solid Films **518**, 1180 (2009).
[10] F.S. de Vicente *et al.*, Brazilian Journal of Physics **25**, 24 (2006).
[11] S. Ulucan *et al.*, Journal of Optoelectronics and Advanced Materials **7**, 297 (2005).
[12] M. Mallak *et al.*, Thin Solid Films **515**, 8072 (2007).
[13] C.H. Heo *et al.*, Thin Solid Films **475**, 183 (2005).
[14] L. Chen *et al.*, Thin Solid Films **515**, 1176 (2006).
[15] J.T. Yates, Jr., Surface Science **603**, 1605 (2009).